




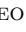
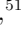















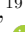
















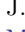













## Search for neutrino doublets and triplets using 11.4 years of IceCube data

R. ABBASI <sup>17</sup>, M. ACKERMANN <sup>65</sup>, J. ADAMS <sup>18</sup>, S. K. AGARWALLA <sup>40</sup>, \* J. A. AGUILAR <sup>11</sup>, M. AHLERS <sup>22</sup>,  
J.M. ALAMEDDINE <sup>23</sup>, N. M. AMIN <sup>44</sup>, K. ANDEEN <sup>42</sup>, C. ARGÜELLES <sup>14</sup>, Y. ASHIDA <sup>53</sup>, S. ATHANASIADOU <sup>65</sup>,  
S. N. AXANI <sup>44</sup>, R. BABU <sup>24</sup>, X. BAI <sup>50</sup>, A. BALAGOPAL V. <sup>40</sup>, M. BARICEVIC <sup>40</sup>, S. W. BARWICK <sup>30</sup>, S. BASH <sup>27</sup>,  
V. BASU <sup>40</sup>, R. BAY <sup>7</sup>, J. J. BEATTY <sup>20,21</sup>, J. BECKER TJUS <sup>10</sup>, † J. BEISE <sup>63</sup>, C. BELLENGHI <sup>27</sup>, S. BENZVI <sup>52</sup>,  
D. BERLEY <sup>19</sup>, E. BERNARDINI <sup>48</sup>, D. Z. BESSON <sup>36</sup>, E. BLAUFUSS <sup>19</sup>, L. BLOOM <sup>60</sup>, S. BLOT <sup>65</sup>, F. BONTEMPO <sup>31</sup>,  
J. Y. BOOK MOTZKIN <sup>14</sup>, C. BOSCOLO MENEGUOLO <sup>48</sup>, S. BÖSER <sup>41</sup>, O. BOTNER <sup>63</sup>, J. BÖTTCHER <sup>1</sup>, J. BRAUN <sup>40</sup>,  
B. BRINSON <sup>5</sup>, Z. BRISSON-TSAVOUSSIS <sup>33</sup>, J. BROSTEAN-KAISER <sup>65</sup>, L. BRUSA <sup>1</sup>, R. T. BURLEY <sup>2</sup>, D. BUTTERFIELD <sup>40</sup>,  
M. A. CAMPANA <sup>49</sup>, I. CARACAS <sup>41</sup>, K. CARLONI <sup>14</sup>, J. CARPIO <sup>34,35</sup>, S. CHATTOPADHYAY <sup>40</sup>, \* N. CHAU <sup>11</sup>, Z. CHEN <sup>56</sup>,  
D. CHIRKIN <sup>40</sup>, S. CHOI <sup>57,58</sup>, B. A. CLARK <sup>19</sup>, A. COLEMAN <sup>63</sup>, P. COLEMAN <sup>1</sup>, G. H. COLLIN <sup>15</sup>, A. CONNOLLY <sup>20,21</sup>,  
J. M. CONRAD <sup>15</sup>, R. CORLEY <sup>53</sup>, D. F. COWEN <sup>61,62</sup>, C. DE CLERCQ <sup>12</sup>, J. J. DELAUNAY <sup>60</sup>, D. DELGADO <sup>14</sup>,  
S. DENG <sup>1</sup>, A. DESAI <sup>40</sup>, P. DESIATI <sup>40</sup>, K. D. DE VRIES <sup>12</sup>, G. DE WASSEIGE <sup>37</sup>, T. DEYOUNG <sup>24</sup>, A. DIAZ <sup>15</sup>,  
J. C. DÍAZ-VÉLEZ <sup>40</sup>, P. DIERICHS <sup>1</sup>, M. DITTMER <sup>43</sup>, A. DOMI <sup>26</sup>, L. DRAPER <sup>53</sup>, H. DUJMOVIC <sup>40</sup>, D. DURNFORD <sup>25</sup>,  
K. DUTTA <sup>41</sup>, M. A. DUVERNOIS <sup>40</sup>, T. EHRHARDT <sup>41</sup>, L. EIDENSCHINK <sup>27</sup>, A. EIMER <sup>26</sup>, P. ELLER <sup>27</sup>, E. ELLINGER <sup>64</sup>,  
S. EL MENTAWI <sup>1</sup>, D. ELSÄSSER <sup>23</sup>, R. ENGEL <sup>31,32</sup>, H. ERPENBECK <sup>40</sup>, W. ESMAIL <sup>43</sup>, J. EVANS <sup>19</sup>, P. A. EVENSON <sup>44</sup>,  
K. L. FAN <sup>19</sup>, K. FANG <sup>40</sup>, K. FARRAG <sup>16</sup>, A. R. FAZELY <sup>6</sup>, A. FEDYNITCH <sup>59</sup>, N. FEIGL <sup>9</sup>, S. FIELDSCHUSTER <sup>26</sup>,  
C. FINLEY <sup>55</sup>, L. FISCHER <sup>65</sup>, D. FOX <sup>61</sup>, A. FRANCKOWIAK <sup>10</sup>, S. FUKAMI <sup>65</sup>, P. FÜRST <sup>1</sup>, J. GALLAGHER <sup>39</sup>,  
E. GANSTER <sup>1</sup>, A. GARCIA <sup>14</sup>, M. GARCIA <sup>44</sup>, G. GARG <sup>40</sup>, \* E. GENTON <sup>14,37</sup>, L. GERHARDT <sup>8</sup>, A. GHADIMI <sup>60</sup>,  
C. GIRARD-CARILLO <sup>41</sup>, C. GLASER <sup>63</sup>, T. GLÜSENKAMP <sup>26,63</sup>, J. G. GONZALEZ <sup>44</sup>, S. GOSWAMI <sup>34,35</sup>, A. GRANADOS <sup>24</sup>,  
D. GRANT <sup>13</sup>, S. J. GRAY <sup>19</sup>, S. GRIFFIN <sup>40</sup>, S. GRISWOLD <sup>52</sup>, K. M. GROTH <sup>22</sup>, D. GUEVEL <sup>40</sup>, C. GÜNTHER <sup>1</sup>,  
P. GUTJAHR <sup>23</sup>, C. HA <sup>54</sup>, C. HAACK <sup>26</sup>, A. HALLGREN <sup>63</sup>, L. HALVE <sup>1</sup>, F. HALZEN <sup>40</sup>, L. HAMACHER <sup>1</sup>,  
H. HAMDAR <sup>56</sup>, M. HA MINH <sup>27</sup>, M. HANDT <sup>1</sup>, K. HANSON <sup>40</sup>, J. HARDIN <sup>15</sup>, A. A. HARNISCH <sup>24</sup>, P. HATCH <sup>33</sup>,  
A. HAUNGS <sup>31</sup>, J. HÄUSSLER <sup>1</sup>, K. HELBING <sup>64</sup>, J. HELLRUNG <sup>10</sup>, J. HERMANNSGABNER <sup>1</sup>, L. HEUERMANN <sup>1</sup>,  
N. HEYER <sup>63</sup>, S. HICKFORD <sup>64</sup>, A. HIDVEGI <sup>55</sup>, C. HILL <sup>16</sup>, G. C. HILL <sup>2</sup>, R. HMAID <sup>16</sup>, K. D. HOFFMAN <sup>19</sup>, S. HORI <sup>40</sup>,  
K. HOSHINA <sup>40</sup>, † M. HOSTERT <sup>14</sup>, W. HOU <sup>31</sup>, T. HUBER <sup>31</sup>, K. HULTQVIST <sup>55</sup>, M. HÜNNEFELD <sup>40</sup>, R. HUSSAIN <sup>40</sup>,  
K. HYMON <sup>23,59</sup>, A. ISHIHARA <sup>16</sup>, W. IWAKIRI <sup>16</sup>, M. JACQUART <sup>40</sup>, S. JAIN <sup>40</sup>, O. JANIK <sup>26</sup>, M. JANSSON <sup>57</sup>,  
M. JEONG <sup>53</sup>, M. JIN <sup>14</sup>, B. J. P. JONES <sup>4</sup>, N. KAMP <sup>14</sup>, D. KANG <sup>31</sup>, W. KANG <sup>57</sup>, X. KANG <sup>49</sup>, A. KAPPES <sup>43</sup>,  
D. KAPPESSER <sup>41</sup>, L. KARDUM <sup>23</sup>, T. KARG <sup>65</sup>, M. KARL <sup>27</sup>, A. KARLE <sup>40</sup>, A. KATIL <sup>25</sup>, U. KATZ <sup>26</sup>, M. KAUER <sup>40</sup>,  
J. L. KELLEY <sup>40</sup>, M. KHANAL <sup>53</sup>, A. KHATEE ZATHUL <sup>40</sup>, A. KHEIRANDISH <sup>34,35</sup>, J. KIRYLUK <sup>56</sup>, S. R. KLEIN <sup>7,8</sup>,  
Y. KOBAYASHI <sup>16</sup>, A. KOCHOCKI <sup>24</sup>, R. KOIRALA <sup>44</sup>, H. KOLANOSKI <sup>9</sup>, T. KONTRIMAS <sup>27</sup>, L. KÖPKE <sup>41</sup>,  
C. KOPPER <sup>26</sup>, D. J. KOSKINEN <sup>22</sup>, P. KOUNDAL <sup>44</sup>, M. KOWALSKI <sup>9,65</sup>, T. KOZYNETS <sup>22</sup>, N. KRIEGER <sup>10</sup>,  
J. KRISHNAMOORTHY <sup>40</sup>, \* T. KRISHNAN <sup>14</sup>, K. KRUISWIJK <sup>37</sup>, E. KRUPCZAK <sup>24</sup>, A. KUMAR <sup>65</sup>, E. KUN <sup>10</sup>,  
N. KURAHASHI <sup>49</sup>, N. LAD <sup>65</sup>, C. LAGUNAS GUALDA <sup>27</sup>, M. LAMOUREUX <sup>37</sup>, M. J. LARSON <sup>19</sup>, F. LAUBER <sup>64</sup>,  
J. P. LAZAR <sup>37</sup>, K. LEONARD DEHOLTON <sup>62</sup>, A. LESZCZYŃSKA <sup>44</sup>, J. LIAO <sup>5</sup>, M. LINCETTO <sup>10</sup>, Y. T. LIU <sup>62</sup>,  
M. LIUBARSKA <sup>25</sup>, C. LOVE <sup>49</sup>, L. LU <sup>40</sup>, F. LUCARELLI <sup>28</sup>, W. LUSZCZAK <sup>20,21</sup>, Y. LYU <sup>7,8</sup>, J. MADSEN <sup>40</sup>,  
E. MAGNUS <sup>12</sup>, K. B. M. MAHN <sup>24</sup>, Y. MAKINO <sup>40</sup>, E. MANAO <sup>27</sup>, S. MANCINA <sup>48</sup>, A. MAND <sup>40</sup>, W. MARIE SAINTE <sup>40</sup>,  
I. C. MARIŞ <sup>11</sup>, S. MARKA <sup>46</sup>, Z. MARKA <sup>46</sup>, M. MARSEE <sup>60</sup>, I. MARTINEZ-SOLER <sup>14</sup>, R. MARUYAMA <sup>45</sup>,  
F. MAYHEW <sup>24</sup>, F. McNALLY <sup>38</sup>, J. V. MEAD <sup>22</sup>, K. MEAGHER <sup>40</sup>, S. MECHBAL <sup>65</sup>, A. MEDINA <sup>21</sup>, M. MEIER <sup>16</sup>,  
Y. MERCKX <sup>12</sup>, L. MERTEN <sup>10</sup>, J. MITCHELL <sup>6</sup>, T. MONTARULI <sup>28</sup>, R. W. MOORE <sup>25</sup>, Y. MORII <sup>16</sup>, R. MORSE <sup>40</sup>,  
M. MOULAI <sup>40</sup>, T. MUKHERJEE <sup>31</sup>, R. NAAB <sup>65</sup>, M. NAKOS <sup>40</sup>, U. NAUMANN <sup>64</sup>, J. NECKER <sup>65</sup>, A. NEGI <sup>4</sup>,  
L. NESTE <sup>55</sup>, M. NEUMANN <sup>43</sup>, H. NIEDERHAUSEN <sup>24</sup>, M. U. NISA <sup>24</sup>, K. NODA <sup>16</sup>, A. NOELL <sup>1</sup>, A. NOVIKOV <sup>44</sup>,  
A. OBERTACKE POLLMANN <sup>16</sup>, V. O'DELL <sup>40</sup>, A. OLIVAS <sup>19</sup>, R. ORSOE <sup>27</sup>, J. OSBORN <sup>40</sup>, E. O'SULLIVAN <sup>63</sup>,  
V. PALUSOVA <sup>41</sup>, H. PANDYA <sup>44</sup>, N. PARK <sup>33</sup>, G. K. PARKER <sup>4</sup>, V. PARRISH <sup>24</sup>, E. N. PAUDEL <sup>44</sup>, L. PAUL <sup>50</sup>,  
C. PÉREZ DE LOS HEROS <sup>63</sup>, T. PERNICE <sup>65</sup>, J. PETERSON <sup>40</sup>, A. PIZZUTO <sup>40</sup>, M. PLUM <sup>50</sup>, A. PONTÉN <sup>63</sup>,  
Y. POPOVYCH <sup>41</sup>, M. PRADO RODRIGUEZ <sup>40</sup>, B. PRIES <sup>24</sup>, R. PROCTER-MURPHY <sup>19</sup>, G. T. PRZYBYLSKI <sup>8</sup>, L. PYRAS <sup>53</sup>,  
C. RAAB <sup>37</sup>, J. RACK-HELLEIS <sup>41</sup>, N. RAD <sup>65</sup>, M. RAVN <sup>3</sup>, K. RAWLINS <sup>3</sup>, Z. RECHAV <sup>40</sup>, A. REHMAN <sup>44</sup>,  
E. RESCONI <sup>27</sup>, S. REUSCH <sup>65</sup>, W. RHODE <sup>23</sup>, B. RIEDEL <sup>40</sup>, A. RIFAIE <sup>64</sup>, E. J. ROBERTS <sup>2</sup>, S. ROBERTSON <sup>7,8</sup>,  
S. RODAN <sup>57,58</sup>, M. RONGEN <sup>26</sup>, A. ROSTED <sup>16</sup>, C. ROTT <sup>53,57</sup>, T. RUHE <sup>23</sup>, L. RUOHAN <sup>27</sup>, D. RYCKBOSCH <sup>29</sup>,  
I. SAFA <sup>40</sup>, J. SAFFER <sup>32</sup>, D. SALAZAR-GALLEGOS <sup>24</sup>, P. SAMPATHKUMAR <sup>31</sup>, A. SANDROCK <sup>64</sup>, M. SANTANDER <sup>60</sup>,  
S. SARKAR <sup>25</sup>, S. SARKAR <sup>47</sup>, J. SAVALBERG <sup>1</sup>, P. SAVINA <sup>40</sup>, P. SCHAILE <sup>27</sup>, M. SCHAUFEL <sup>1</sup>, H. SCHIELER <sup>31</sup>,  
S. SCHINDLER <sup>26</sup>, L. SCHLICKMANN <sup>41</sup>, B. SCHLÜTER <sup>43</sup>, F. SCHLÜTER <sup>11</sup>, N. SCHMEISSER <sup>64</sup>, T. SCHMIDT <sup>19</sup>

J. SCHNEIDER <sup>26</sup> F. G. SCHRÖDER <sup>31,44</sup> L. SCHUMACHER <sup>26</sup> S. SCHWIRN,<sup>1</sup> S. SCLAFANI <sup>19</sup> D. SECKEL,<sup>44</sup>  
 L. SEEN <sup>40</sup> M. SEIKH <sup>36</sup> M. SEO,<sup>57</sup> S. SEUNARINE <sup>51</sup> P. SEVLE MYHR <sup>37</sup> R. SHAH <sup>49</sup> S. SHEFALI,<sup>32</sup>  
 N. SHIMIZU <sup>16</sup> M. SILVA <sup>40</sup> B. SKRZYPEK <sup>7</sup> B. SMITHERS <sup>4</sup> R. SNIHUR,<sup>40</sup> J. SOEDINGREKSO,<sup>23</sup> A. SØGAARD,<sup>22</sup>  
 D. SOLDIN <sup>53</sup> P. SOLDIN <sup>1</sup> G. SOMMANI <sup>10</sup> C. SPANNFELLNER,<sup>27</sup> G. M. SPICZAK <sup>51</sup> C. SPIERING <sup>65</sup>  
 J. STACHURSKA <sup>29</sup> M. STAMATIKOS,<sup>21</sup> T. STANEV,<sup>44</sup> T. STEZELBERGER <sup>8</sup> T. STÜRWARD,<sup>64</sup> T. STUTTARD <sup>22</sup>  
 G. W. SULLIVAN <sup>19</sup> I. TABOADA <sup>5</sup> S. TER-ANTONYAN <sup>6</sup> A. TERLIUK,<sup>27</sup> M. THIESMEYER <sup>40</sup> W. G. THOMPSON <sup>14</sup>  
 J. THWAITES <sup>40</sup> S. TILAV,<sup>44</sup> K. TOLLEFSON <sup>24</sup> C. TÖNNIS,<sup>57</sup> S. TOSCANO <sup>11</sup> D. TOSI,<sup>40</sup> A. TRETTIN,<sup>65</sup>  
 M. A. UNLAND ELORRIETA <sup>43</sup> A. K. UPADHYAY <sup>40,\*</sup> K. UPSHAW,<sup>6</sup> A. VAIDYANATHAN,<sup>42</sup> N. VALTONEN-MATTILA <sup>63</sup>  
 J. VANDENBROUCKE <sup>40</sup> N. VAN EIJDHOVEN <sup>12</sup> D. VANNEROM,<sup>15</sup> J. VAN SANTEN <sup>65</sup> J. VARA,<sup>43</sup> F. VARSÌ,<sup>32</sup>  
 J. VEITCH-MICHAELIS,<sup>40</sup> M. VENUGOPAL,<sup>31</sup> M. VEREecken,<sup>37</sup> S. VERGARA CARRASCO,<sup>18</sup> S. VERPOEST <sup>44</sup> D. VESKE,<sup>46</sup>  
 A. VIJAI,<sup>19</sup> C. WALCK,<sup>55</sup> A. WANG <sup>5</sup> C. WEAVER <sup>24</sup> P. WEIGEL,<sup>15</sup> A. WEINDL,<sup>31</sup> J. WELDERT,<sup>62</sup> A. Y. WEN <sup>14</sup>  
 C. WENDT <sup>40</sup> J. WERTHEBACH,<sup>23</sup> M. WEYRAUCH,<sup>31</sup> N. WHITEHORN <sup>24</sup> C. H. WIEBUSCH <sup>1</sup> D. R. WILLIAMS,<sup>60</sup>  
 L. WITTHAUS <sup>23</sup> M. WOLF <sup>27</sup> G. WREDE,<sup>26</sup> X. W. XU,<sup>6</sup> J. P. YANEZ,<sup>25</sup> E. YILDIZCI,<sup>40</sup> S. YOSHIDA <sup>16</sup> R. YOUNG,<sup>36</sup>  
 F. YU <sup>14</sup> S. YU <sup>53</sup> T. YUAN <sup>40</sup> A. ZEGARELI <sup>10</sup> S. ZHANG <sup>24</sup> Z. ZHANG,<sup>56</sup> P. ZHELNIN <sup>14</sup> P. ZILBERMAN<sup>40</sup>  
 AND M. ZIMMERMAN<sup>40</sup>

ICECUBE COLLABORATION

<sup>1</sup>*III. Physikalisches Institut, RWTH Aachen University, D-52056 Aachen, Germany*

<sup>2</sup>*Department of Physics, University of Adelaide, Adelaide, 5005, Australia*

<sup>3</sup>*Dept. of Physics and Astronomy, University of Alaska Anchorage, 3211 Providence Dr., Anchorage, AK 99508, USA*

<sup>4</sup>*Dept. of Physics, University of Texas at Arlington, 502 Yates St., Science Hall Rm 108, Box 19059, Arlington, TX 76019, USA*

<sup>5</sup>*School of Physics and Center for Relativistic Astrophysics, Georgia Institute of Technology, Atlanta, GA 30332, USA*

<sup>6</sup>*Dept. of Physics, Southern University, Baton Rouge, LA 70813, USA*

<sup>7</sup>*Dept. of Physics, University of California, Berkeley, CA 94720, USA*

<sup>8</sup>*Lawrence Berkeley National Laboratory, Berkeley, CA 94720, USA*

<sup>9</sup>*Institut für Physik, Humboldt-Universität zu Berlin, D-12489 Berlin, Germany*

<sup>10</sup>*Fakultät für Physik & Astronomie, Ruhr-Universität Bochum, D-44780 Bochum, Germany*

<sup>11</sup>*Université Libre de Bruxelles, Science Faculty CP230, B-1050 Brussels, Belgium*

<sup>12</sup>*Vrije Universiteit Brussel (VUB), Dienst ELEM, B-1050 Brussels, Belgium*

<sup>13</sup>*Dept. of Physics, Simon Fraser University, Burnaby, BC V5A 1S6, Canada*

<sup>14</sup>*Department of Physics and Laboratory for Particle Physics and Cosmology, Harvard University, Cambridge, MA 02138, USA*

<sup>15</sup>*Dept. of Physics, Massachusetts Institute of Technology, Cambridge, MA 02139, USA*

<sup>16</sup>*Dept. of Physics and The International Center for Hadron Astrophysics, Chiba University, Chiba 263-8522, Japan*

<sup>17</sup>*Department of Physics, Loyola University Chicago, Chicago, IL 60660, USA*

<sup>18</sup>*Dept. of Physics and Astronomy, University of Canterbury, Private Bag 4800, Christchurch, New Zealand*

<sup>19</sup>*Dept. of Physics, University of Maryland, College Park, MD 20742, USA*

<sup>20</sup>*Dept. of Astronomy, Ohio State University, Columbus, OH 43210, USA*

<sup>21</sup>*Dept. of Physics and Center for Cosmology and Astro-Particle Physics, Ohio State University, Columbus, OH 43210, USA*

<sup>22</sup>*Niels Bohr Institute, University of Copenhagen, DK-2100 Copenhagen, Denmark*

<sup>23</sup>*Dept. of Physics, TU Dortmund University, D-44221 Dortmund, Germany*

<sup>24</sup>*Dept. of Physics and Astronomy, Michigan State University, East Lansing, MI 48824, USA*

<sup>25</sup>*Dept. of Physics, University of Alberta, Edmonton, Alberta, T6G 2E1, Canada*

<sup>26</sup>*Erlangen Centre for Astroparticle Physics, Friedrich-Alexander-Universität Erlangen-Nürnberg, D-91058 Erlangen, Germany*

<sup>27</sup>*Physik-department, Technische Universität München, D-85748 Garching, Germany*

<sup>28</sup>*Département de physique nucléaire et corpusculaire, Université de Genève, CH-1211 Genève, Switzerland*

<sup>29</sup>*Dept. of Physics and Astronomy, University of Gent, B-9000 Gent, Belgium*

<sup>30</sup>*Dept. of Physics and Astronomy, University of California, Irvine, CA 92697, USA*

<sup>31</sup>*Karlsruhe Institute of Technology, Institute for Astroparticle Physics, D-76021 Karlsruhe, Germany*

<sup>32</sup>*Karlsruhe Institute of Technology, Institute of Experimental Particle Physics, D-76021 Karlsruhe, Germany*

<sup>33</sup>*Dept. of Physics, Engineering Physics, and Astronomy, Queen's University, Kingston, ON K7L 3N6, Canada*

<sup>34</sup>*Department of Physics & Astronomy, University of Nevada, Las Vegas, NV 89154, USA*

<sup>35</sup>*Nevada Center for Astrophysics, University of Nevada, Las Vegas, NV 89154, USA*

<sup>36</sup>*Dept. of Physics and Astronomy, University of Kansas, Lawrence, KS 66045, USA*

<sup>37</sup>*Centre for Cosmology, Particle Physics and Phenomenology - CP3, Université catholique de Louvain, Louvain-la-Neuve, Belgium*

<sup>38</sup>*Department of Physics, Mercer University, Macon, GA 31207-0001, USA*

<sup>39</sup>*Dept. of Astronomy, University of Wisconsin—Madison, Madison, WI 53706, USA*

<sup>40</sup>*Dept. of Physics and Wisconsin IceCube Particle Astrophysics Center, University of Wisconsin—Madison, Madison, WI 53706, USA*

<sup>41</sup>*Institute of Physics, University of Mainz, Staudinger Weg 7, D-55099 Mainz, Germany*

<sup>42</sup>*Department of Physics, Marquette University, Milwaukee, WI 53201, USA*

<sup>43</sup>*Institut für Kernphysik, Universität Münster, D-48149 Münster, Germany*

<sup>44</sup>*Bartol Research Institute and Dept. of Physics and Astronomy, University of Delaware, Newark, DE 19716, USA*

<sup>45</sup>*Dept. of Physics, Yale University, New Haven, CT 06520, USA*

<sup>46</sup>*Columbia Astrophysics and Nevis Laboratories, Columbia University, New York, NY 10027, USA*

<sup>47</sup>*Dept. of Physics, University of Oxford, Parks Road, Oxford OX1 3PU, United Kingdom*

<sup>48</sup>*Dipartimento di Fisica e Astronomia Galileo Galilei, Università Degli Studi di Padova, I-35122 Padova PD, Italy*

<sup>49</sup>*Dept. of Physics, Drexel University, 3141 Chestnut Street, Philadelphia, PA 19104, USA*

<sup>50</sup>*Physics Department, South Dakota School of Mines and Technology, Rapid City, SD 57701, USA*

<sup>51</sup>*Dept. of Physics, University of Wisconsin, River Falls, WI 54022, USA*

<sup>52</sup>*Dept. of Physics and Astronomy, University of Rochester, Rochester, NY 14627, USA*

<sup>53</sup>*Department of Physics and Astronomy, University of Utah, Salt Lake City, UT 84112, USA*

<sup>54</sup>*Dept. of Physics, Chung-Ang University, Seoul 06974, Republic of Korea*

<sup>55</sup>*Oskar Klein Centre and Dept. of Physics, Stockholm University, SE-10691 Stockholm, Sweden*

<sup>56</sup>*Dept. of Physics and Astronomy, Stony Brook University, Stony Brook, NY 11794-3800, USA*

<sup>57</sup>*Dept. of Physics, Sungkyunkwan University, Suwon 16419, Republic of Korea*

<sup>58</sup>*Institute of Basic Science, Sungkyunkwan University, Suwon 16419, Republic of Korea*

<sup>59</sup>*Institute of Physics, Academia Sinica, Taipei, 11529, Taiwan*

<sup>60</sup>*Dept. of Physics and Astronomy, University of Alabama, Tuscaloosa, AL 35487, USA*

<sup>61</sup>*Dept. of Astronomy and Astrophysics, Pennsylvania State University, University Park, PA 16802, USA*

<sup>62</sup>*Dept. of Physics, Pennsylvania State University, University Park, PA 16802, USA*

<sup>63</sup>*Dept. of Physics and Astronomy, Uppsala University, Box 516, SE-75120 Uppsala, Sweden*

<sup>64</sup>*Dept. of Physics, University of Wuppertal, D-42119 Wuppertal, Germany*

<sup>65</sup>*Deutsches Elektronen-Synchrotron DESY, Platanenallee 6, D-15738 Zeuthen, Germany*

(Dated: January 17, 2025)

## ABSTRACT

We report a search for high-energy astrophysical neutrino multiplets, detections of multiple neutrino clusters in the same direction within 30 days, based on an analysis of 11.4 years of IceCube data. A new search method optimized for transient neutrino emission with a monthly time scale is employed, providing a higher sensitivity to neutrino fluxes. This result is sensitive to neutrino transient emission, reaching per-flavor flux of approximately  $10^{-10}$  erg cm<sup>-2</sup> sec<sup>-1</sup> from the Northern sky in the energy range  $E \gtrsim 50$  TeV. The number of doublets and triplets identified in this search is compatible with the atmospheric background hypothesis, which leads us to set limits on the nature of neutrino transient sources with emission timescales of one month.

*Keywords:* Neutrino astronomy(1100) — Neutrino telescopes(1105) — Optical astronomy(1776)

## 1. INTRODUCTION

The IceCube Neutrino Observatory discovered a diffuse flux of high-energy astrophysical neutrinos

in 2013 (Aartsen et al. 2013). The observed flux per neutrino flavor is at the level of  $\phi_\nu \sim 10^{-18}$  GeV<sup>-1</sup> cm<sup>-2</sup> sec<sup>-1</sup> sr<sup>-1</sup> at  $E_\nu = 100$  TeV with a spectral index between 2.4 and 2.9 depending on various neutrino selections (Abbasi et al. 2022a; Aartsen et al. 2020, 2021a; Abbasi et al. 2021). Hereafter, a flux implicitly represents the sum of neutrinos and antineutrinos unless otherwise stated.

The origin of the diffuse flux is uncertain, but there are various hints from the studies of the individual point source searches. In 2017, the association of a real-time

\* also at Institute of Physics, Sachivalaya Marg, Sainik School Post, Bhubaneswar 751005, India

† also at Department of Space, Earth and Environment, Chalmers University of Technology, 412 96 Gothenburg, Sweden

‡ also at Earthquake Research Institute, University of Tokyo, Bunkyo, Tokyo 113-0032, Japan

neutrino alert (IceCube-170922A) with a high-energy gamma-ray flare observed by Fermi-LAT (Aartsen et al. 2018) suggested that a blazar TXS 0506+056 was likely a source of high-energy neutrinos. However, blazars cannot explain all of the diffuse flux observed by IceCube (Aartsen et al. 2017b). In 2022, the nearby active galaxy NGC 1068 was identified as a neutrino source by an excess of neutrinos with energies of 1.5-15 TeV above backgrounds with significance of  $4.2\sigma$  (Abbasi et al. 2022b). In 2023, neutrino emission from the galactic plane was reported at  $4.5\sigma$  significance (Abbasi et al. 2023a), but this only contributes to 6-13% of the isotropic diffuse flux at 30 TeV.

Astrophysical transient phenomena with a time scale of weeks to months have been proposed as neutrino sources. For example, a subclass of core-collapse supernovae (CCSNe) radiates  $\mathcal{O}(100)$  brighter than standard SNe, possibly due to interactions between the ejecta and dense circumstellar materials (Moriya et al. 2018; Gal-Yam 2019). In such environments, along with the prompt emission of MeV energy neutrinos, efficient generation of 1-100 TeV neutrinos can occur over a timescale of up to 100 days (Murase et al. 2011; Kheirandish & Murase 2023; Pitik et al. 2023; Murase 2018). Tidal disruption events (TDEs) are observed by their lasting several months emission of optical radiation. High-energy neutrino emission from TDEs was predicted to react a total bolometric energy of  $\mathcal{O}(10^{54})$  erg (Hayasaki & Yamazaki 2019; Murase et al. 2020; Winter & Lunardini 2023). Furthermore, Stein et al. (2021) reported a possible association between IceCube real-time neutrino alerts and TDE flares.

A search for multiple neutrinos originating from the same direction within a timescale of one month is a straightforward method for capturing these phenomena. If these transient sources contribute to the diffuse neutrino flux, the detection of neutrino *multiplets* can identify sources and extract the characteristics of the source population. For transient sources of burst rate density  $\rho_\nu$  with all-flavor neutrino isotropic emission energy per source,  $\mathcal{E}_\nu$ , the diffuse flux scales approximately as  $E_\nu^2 \phi_\nu \propto \mathcal{E}_\nu \rho_\nu$  while the detection rate of doublets is approximately proportional to  $\mathcal{E}_\nu^2 \rho_\nu$ . Thus, the search for doublets (and multiplets in general) is more sensitive to a population of bright (*i.e.*, higher  $\mathcal{E}_\nu$ ), and rarer (*i.e.*, lower  $\rho_\nu$ ) transient sources. Furthermore, a null detection of astrophysical neutrino multiplets constrains these parameters and can rule out candidate transient sources for the diffuse flux (Kowalski & Mohr 2007; Aartsen et al. 2019; Yoshida et al. 2022).

We report here a search for neutrino doublets and triplets using IceCube data. The search scheme is op-

timized for a relatively long transient time scale of 30 days. This is different from our previous doublet search (Aartsen et al. 2019), where the search was conducted for short transient with less than 100 s, corresponding to a much faster emission process such as gamma-ray bursts (GRBs).

The remainder of this paper is organized as follows. Sec. 2 explains IceCube observatory and the selection method for neutrino events for this analysis. In Sec. 3 presents the analysis method of the multiplets, together with its sensitivity. Sec. 4 presents the results of our analysis of the dataset. Sec. 5 discusses the outcomes of the main results. We also report a correlation analysis between multiplets and X-ray data recorded by the Monitor of All-sky X-ray Images (MAXI). Finally, in Sec. 6, we summarize the conclusions of the search for multiplets.

## 2. THE ICECUBE OBSERVATORY

The IceCube observatory at the South Pole is a cubic-kilometer detector for astrophysical neutrinos (Aartsen et al. 2017a; Abbasi et al. 2009). Cherenkov emission from charged particles generated by the interaction of high-energy neutrinos are observed using 5160 digital optical modules (DOMs). The DOMs host 10" photomultiplier tubes in a high-pressure-resistant vessel (Abbasi et al. 2010) and were deployed between 1450 and 2450 m below the surface of the ice on 86 vertical strings. The detected photon signals are sent to the surface IceCube laboratory, and recorded when the trigger condition is satisfied. The patterns of photons detected from neutrino events are predominantly classified as either *tracks* or *cascades*. A track event can be initiated by the charged current interaction of  $\nu_\mu$ , and the photons disperse along the path of the outgoing muon, providing good angular resolution, typically less than  $1^\circ$  for high energy ( $\gtrsim 10$  TeV) neutrinos. A cascade event is initiated by charged-current interactions of  $\nu_e$  and  $\nu_\tau$ , or neutral-current interactions of all neutrino flavors. Its photon distribution exhibits more isotropic quasi-pointlike patterns, resulting in a poorer resolution than that of a track event.

The event set used in this study is referred to as the *GFU sample* (Kintscher 2020; Aartsen et al. 2016a), which contains high-quality track events with excellent pointing accuracy. The dataset was collected from the completion of IceCube in 2011 until the end of 2022, corresponding to a total live time of 11.4 years when accounting for data quality selections. The total number of selected events is  $N = 1,212,746$ , and the event rate is 3.4 mHz. The sample is also used to issue single high-energy track neutrino alerts (Abbasi et al. 2023b).



Neutrino events are further selected based on their reconstructed muon energies (Abbasi et al. 2013) and directions (Ahrens et al. 2004). This study utilized only the track type events in the northern direction with  $\delta > -5^\circ$ , forming the *Northern Sky GFU* sample. The main background originates from atmospheric neutrinos and dominates by 99.7%. At the South Pole, a one-to-one relationship exists between the declination  $\delta$  and the zenith angle which allows us to characterize the atmospheric background as a function of  $\delta$ .

### 3. MULTIPLETT ANALYSIS

In the following, the emission energy of individual neutrino sources is bolometrically defined in the energy range from 10 TeV to 1 PeV, which is represented as  $\mathcal{E}_\nu^*$ . The expected number of neutrinos passing the event selection from a source at redshift  $z$ ,  $n_\nu(\mathcal{E}_\nu^*, z)$ , yields a probability of multiplet detection as  $\epsilon(\mathcal{E}_\nu^*, z) = 1 - e^{-n_\nu} - n_\nu e^{-n_\nu}$ . The total number of multiplets (doublets, triplets, quadruplets, ..., and so on) expected from the population of such sources across the Universe is given by (Murase & Waxman 2016; Yoshida et al. 2022):

$$N_M = \rho_\nu T_{\text{obs}} \int dV \epsilon(\mathcal{E}_\nu^*, z) \psi(z), \quad (1)$$

where  $T_{\text{obs}}$  is a total live time of observation and  $dV$  is a volume element. The factor  $\psi(z)$  represents an evolution of the source population with redshifts, and in the present analysis,  $\psi(z)$  follows  $(1+z)^{3.4}$  for  $z \leq 1$  and is constant beyond  $z = 1$ . This is comparable to the star formation rate (SFR). For instance, a source population with  $\mathcal{E}_\nu^* = 10^{52}$  erg and  $\rho_\nu = 10^{-8}$  Mpc $^{-3}$  yr $^{-1}$  yields  $N_M \sim 3$  per year for the Northern-sky GFU sample. This number is much lower than the number of combinations of neutrinos due to atmospheric backgrounds (the rate is  $\sim \mathcal{O}(10^5)$  per year). It is necessary to optimize the search method for such a low detection rate of multiplets. Below, we describe our newly developed multiplet finding algorithms and the resultant likelihood construction.

#### 3.1. Selection of event clusters

Any excess of neutrino events above the atmospheric background from a given patch of the sky can be identified by evaluating likelihoods of, both, astrophysical and background hypotheses for the observed events in a sliding search time window. A previous time-dependent point-source search (Kintscher 2020) (hereafter referred to as *time-dependent GFU*) is based on this method using the nested-likelihood technique (Aartsen et al. 2008).

To reduce computation time, we employ a *seeded clustering* method in this analysis. The  $i$ -th event in the sample seeds a search for clustered events in time up to  $T_{\text{max}} = 30$  days prior to the seed event and direction within a  $3^\circ$  opening angle. We then determine every combination of two (*i.e.*, doublets) and three (*i.e.*, triplet) event pairs. This pre-selection method was previously adopted for time-independent searches (Aartsen et al. 2015). We then select the most statistically significant multiplet among all combinations based on a test statistic introduced below. Iterations of this clustering procedure are performed for all seeding events in the sample, separately for doublets and triplets, that generate the potentially interesting series of two pools of doublets and triplets. Note that this algorithm in general permits more than three neutrino events to be multiple pairs of doublets.

The pools of the multiplets are subject to the hypothesis testing by using the following likelihood. For a given doublet and a triplet in the multiplet pools, we define an extended Poisson likelihood of the signal (background) hypothesis as:

$$\mathcal{L}^{\text{sig(bg)}} = \epsilon_{\text{sig(bg)}} \prod_i^{N=2(\text{or}3)} P_{\text{sig(bg)}}^E(E^i) P_{\text{sig(bg)}}^{\vec{n}}(\vec{n}_i), \quad (2)$$

where  $E^i$  is the proxy for the neutrino energy (Abbasi et al. 2013),  $\vec{n}_i$  is the reconstructed direction of an event  $i$ , and  $P_{\text{sig(bg)}}^E$  and  $P_{\text{sig(bg)}}^{\vec{n}}$  are the energy and directional probability density functions (PDFs) for the signal (background) hypothesis. The first term  $\epsilon_{\text{sig(bg)}}$  represents a probability to observe multiplets (more than two background events) in  $1 \text{ deg}^2$  within the time window  $T_{\text{max}}$  at a declination in  $\delta$ , and given by (Yoshida et al. 2022)

$$\epsilon_{\text{sig}} = (1 - e^{-\Delta N_M}) e^{-\Delta \mu_{\text{bg}}}, \quad (3)$$

$$\epsilon_{\text{bg}} = (1 - e^{-\Delta \mu_{\text{bg}} - \Delta \mu_{\text{bg}}} e^{-\Delta \mu_{\text{bg}}}) e^{-\Delta N_M}, \quad (4)$$

where  $\Delta N_M = \Delta N_M(\sin \delta)$  denotes the expected number of multiplets, and  $\Delta \mu_{\text{bg}} = \Delta \mu_{\text{bg}}(\sin \delta)$  denotes the expected number of background events in the same region, solid angle ( $1 \text{ deg}^2$ ), and time window.

The expected number of multiplets  $N_M$  depends on the representative neutrino emission energy,  $\mathcal{E}_\nu^*$ , and local burst rate density,  $\rho_\nu$ . We used a standard-candle source model in which all sources yielding multiplet events are identical across the universe, with universal values for  $\mathcal{E}_\nu^*$  and  $\rho_\nu$ . We use  $\mathcal{E}_\nu^* = 2.1 \times 10^{54}$  erg and  $\rho_\nu = 1.7 \times 10^{-10}$  Mpc $^{-3}$  yr $^{-1}$  as the baseline configuration for the likelihood calculations. We confirmed that the choice of baseline values does not significantly change the resulting sensitivity.

The energy PDF  $P_{\text{sig}}^E$  depends on the neutrino spectral shape. We assume that the emission spectrum follows a single power law,  $E^{-\gamma}$ . The index  $\gamma$  is assumed to be fixed at a baseline value of  $\gamma = 2.3$  (a lower end of the measured spectrum of the diffuse flux by IceCube (Abasi et al. 2022a)). The directional PDF  $P_{\text{sig}}^{\vec{n}}$  relies on the knowledge of the event localization uncertainty. We describe  $P_{\text{sig}}^{\vec{n}}$  by a two-dimensional Gaussian distribution with an error matrix estimated by the fit procedure of the directional reconstruction (Ahrens et al. 2004). The background directional PDF  $P_{\text{bg}}^E$  is assumed to be flat (constant) over a  $3^\circ$  region.

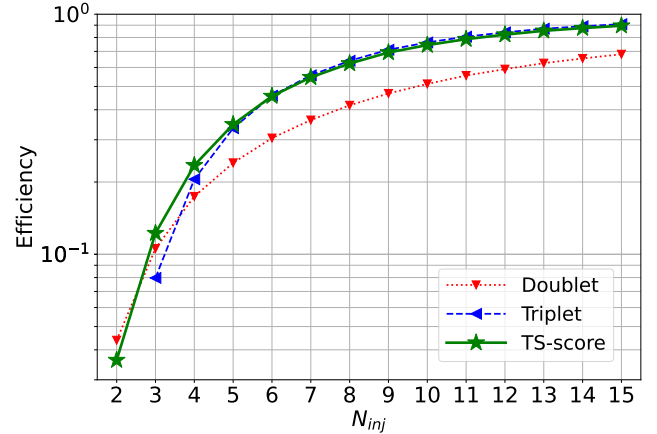
Each identified doublet or triplet is then assigned to the likelihood ratio test statistic

$$\Lambda = 2 \log \frac{\mathcal{L}^{\text{sig}}(\hat{\vec{n}})}{\mathcal{L}^{\text{bg}}}, \quad (5)$$

where  $\hat{\vec{n}}$  is the direction that maximizes the likelihood. The distribution of  $\Lambda$  under the background-only hypothesis yields the p-value or the false alarm rate (FAR) for a given  $\Lambda$  value. The background distribution of  $\Lambda$  for doublets and triplets are obtained by right-ascension scrambling of the control dataset, and exhibit excellent agreement with that of doublets and triplets in the full dataset as described in Sec. 4. To unite doublets and triplets, we introduce a TS-score defined by the  $\Lambda$  value corresponding to the smallest FAR out of the pool of doublets and triplets for every seed event. Thus, the TS-score distribution under the background-only hypothesis provides a unified global p-value or FAR for every seed event.

### 3.2. Signal efficiency

We derive the signal efficiency as the expected fraction of neutrino transients surpassing a TS-score threshold corresponding to  $\text{FAR} < 1 \text{ yr}^{-1}$ , which represents a metric of the effective performance for a discovery for astrophysical multiplet candidates. To evaluate the signal efficiency, we simulate transient neutrino emissions from hypothetical sources. The number of signal neutrino events satisfying the North Sky GFU selection,  $N_{\text{inj}}$ , is introduced here as a proxy for the source luminosity. The neutrino emission follows an  $E^{-2.3}$  spectrum with a flat transient time profile up to  $T_{\text{max}} = 30$  days from 10 TeV to 1 PeV and zero elsewhere. For each signal trial, we inject  $N_{\text{inj}}$  events to the background model prepared by right-ascension scrambling of data. The injected  $N_{\text{inj}}$  neutrino events seed the calculations of  $\Lambda$ , and if any two (three) injected signal events are properly selected as a doublet (triplet) with corresponding FAR satisfying  $< 1 \text{ yr}^{-1}$ , the trial is defined to surpass



**Figure 1.** Signal efficiency as a function of injected number of signal neutrino events for doublet (red), triplet (blue), and TS-score (green). The definition of the efficiency is given in the main text.

the threshold, regardless of the consistency between the fit and true injected directions.

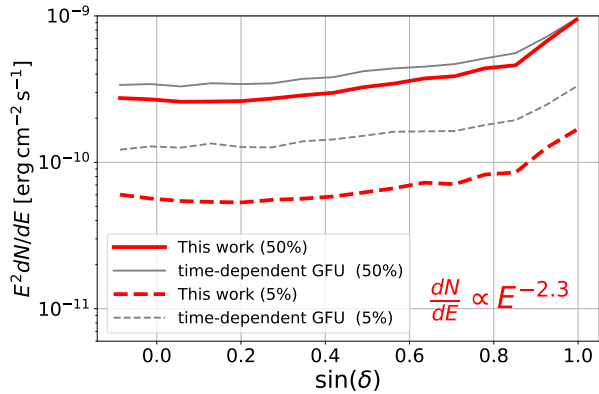
Figure 1 shows the efficiency obtained from these pseudo-experimental trials. We show the resulting efficiencies for  $\text{FAR} < 1 \text{ yr}^{-1}$  by doublet-only, triplet-only, and the combined treatments by the TS-score, respectively, for comparison. Though the magnitude of efficiency for  $N_{\text{inj}} \leq 5$  is small ( $\lesssim 10\%$ ), this provides non-negligible opportunities to discover neutrino multiplets in the populations of relatively dimmer sources. For example, for emissions from sources with  $\mathcal{E}_\nu^* = 10^{52}$  erg distributed across space, approximately 60 % of the detection cases range from  $N_{\text{inj}} = 2$  to 5.

### 3.3. Sensitivity to a multiplet source flux

Figure 2 illustrates the sensitivity of the multiplet source flux to satisfy  $\text{FAR} < 1 \text{ yr}^{-1}$  as a function of the declination. Two cases of 50% and 5% efficiencies are displayed. When 50% of efficiency is required (solid), the presented algorithm shows compatible performance with the time-dependent GFU method, while a factor of  $\sim 2$  improvement is expected for 5% efficiency (dashed). Because less bright sources should be more abundant, the smaller efficiency per source could result in a notable number of detections particularly when we utilize information of multi-messenger coincidences such as archival follow-up analyses or additional observations by alerts. The improvement comes from the contribution of the small number of neutrino detections ( $N_{\text{inj}} \leq 5$ ) explained in Sec. 3.2.

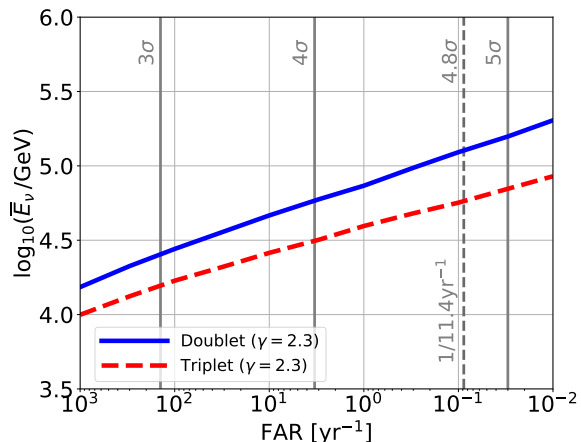
### 3.4. Main energy range

Figure 3 shows the average energies of multiplets for various thresholds of FAR values. At the significance



**Figure 2.** Averaged energy flux (sum of  $\nu_\mu$  and  $\bar{\nu}_\mu$  per flavor) at 100 TeV in  $T_{\max} = 30$  days observed at a significance corresponding to  $\text{FAR} < 1 \text{ yr}^{-1}$  as a function of  $\sin \delta$  for the presented algorithm (red) and time-dependent GFU (gray) when  $\gamma = 2.3$ . The solid and dashed curves represent probabilities of signal detections of 50% and 5%, respectively.

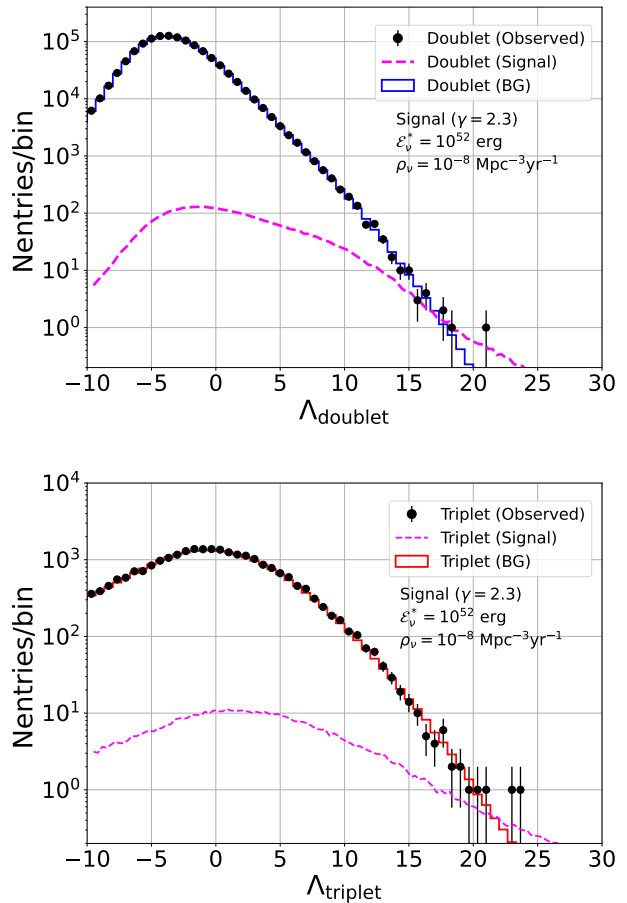
of  $4.8\sigma$  of background trials (corresponding to  $\text{FAR} = 1/11.4\text{yr}$ ), the main neutrino range is  $E \gtrsim 100$  TeV for doublets and  $E \gtrsim 50$  TeV for triplets.



**Figure 3.** Averaged energies of the selected multiplets for various levels of thresholds converted into the corresponding FAR. The energy of the multiplet is the geometric mean of the neutrino energies involved in the multiplets. The solid and dashed curves correspond to doublets and triplets, respectively. The vertical solid lines indicate  $3\sigma$ ,  $4\sigma$ , and  $5\sigma$  of the normalized background distributions, and the dashed-line indicates  $4.8\sigma$  corresponding to  $\text{FAR} = 1/11.4 \text{ yr}$ .

### 3.5. Source localization accuracy

Because of the inclusion of multiple events, the source localization accuracy of multiplets is superior to the angular uncertainty of individual events. Multiplets whose FARs are less than  $1 \text{ yr}^{-1}$  results in an excellent source localization accuracy of  $0.3^\circ$  at 90% containment.



**Figure 4.** Distribution of the test statistics:  $\Lambda_{\text{doublet}}$  (top) and  $\Lambda_{\text{triplet}}$  (bottom). The markers represent observed experimental data, while the solid lines indicate the expected distributions from backgrounds. The magenta dashed lines are the expected distributions of the signal when  $\gamma = 2.3$ ,  $\mathcal{E}_\nu^* = 10^{52} \text{ erg}$ , and  $\rho_\nu = 10^{-8} \text{ Mpc}^{-3} \text{ yr}^{-1}$ . These parameters were arbitrary chosen for illustration.

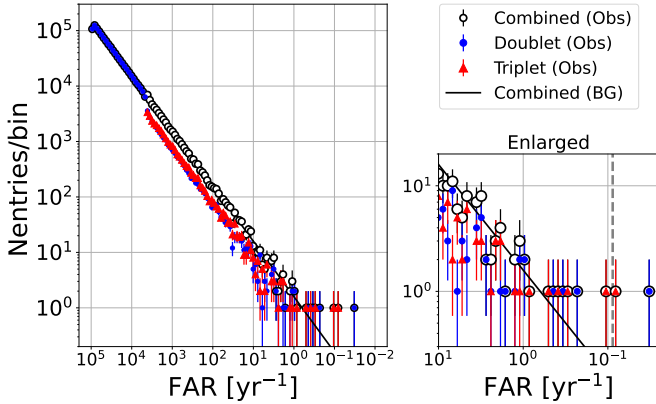
## 4. RESULTS

We search for multiplet signals in the IceCube Northern Sky GFU sample taken from May 2011 to December 2022 after finalizing the selection scheme and confirming its performance following a blinded analysis strategy. No statistically significant doublets or triplets of astrophysical origins are observed. Figure 4 shows the  $\Lambda$  distributions of doublets and triplets showing excellent agreement with the background distributions. For illustrative purposes, we also display the expected distributions by standard-candle neutrino sources with  $\mathcal{E}_\nu^* = 10^{52} \text{ erg}$  and  $\rho_\nu = 10^{-8} \text{ Mpc}^{-3} \text{ yr}^{-1}$ . Figure 5 shows the distribution of FAR values converted from the TS-score.

Table 1 summarizes the 12 most significant multiplets observed in the dataset indexed according to their significance by  $k$ . We select these multiplets with prede-

**Table 1.** Summary of the top 12 significant multiplets observed in the dataset.

Index $k$	Type <sup>a</sup>	Fit RA <sup>b</sup> (deg)	Fit DEC <sup>b</sup> (deg)	$\log_{10}E_1$ (GeV)	$\log_{10}E_2$ (GeV)	$\log_{10}E_3$ (GeV)	MJD <sub>1</sub> <sup>c</sup> (day)	MJD <sub>2</sub> <sup>c</sup> (day)	MJD <sub>3</sub> <sup>c</sup> (day)	$\Delta T$ <sup>d</sup> (day)	Local <sup>e</sup> p-value $\times 10^6$	FAR <sup>e</sup> (yr <sup>-1</sup> )
1	D	110.05	11.05	6.77	3.75	-	56819.20	56813.38	-	5.8	0.32	0.034
2	T	0.58	-0.35	3.62	4.31	5.47	59027.66	59015.46 <sup>+</sup>	59011.22 <sup>*</sup>	16.4	0.74	0.078
3	T	200.53	6.30	3.59	4.34	4.26	56487.55	56459.68 <sup>#</sup>	56458.53 <sup>†</sup>	29	1.1	0.112
4	D	0.58	-0.35	4.31	5.47	-	59015.46 <sup>+</sup>	59011.22 <sup>*</sup>	-	4.2	2.3	0.30
5	T	200.54	6.29	3.69	4.34	4.26	56479.74	56459.68 <sup>#</sup>	56458.53 <sup>†</sup>	21.2	2.9	0.305
6	D	121.15	-2.01	3.94	3.97	-	59260.68	59255.52	-	5.2	3.1	0.326
7	T	0.55	-0.32	3.67	4.31	5.47	59041.22	59015.46 <sup>+</sup>	59011.22 <sup>*</sup>	30	3.8	0.396
8	D	133.75	52.87	4.45	4.48	-	58759.56	58755.30	-	4.3	4.5	0.469
9	T	219.29	12.79	4.61	3.7	5.04	56817.03	56809.62	56794.31	22.7	4.7	0.487
10	T	123.38	8.20	3.77	4.76	4.46	59274.42	59271.67 <sup>‡</sup>	59257.61 <sup>b</sup>	16.8	7.6	0.796
11	D	200.53	6.29	4.34	4.26	-	56459.68 <sup>#</sup>	56458.53 <sup>†</sup>	-	1.2	8.8	0.918
12	D	123.38	8.20	4.76	4.46	-	59271.67 <sup>‡</sup>	59257.61 <sup>b</sup>	-	14.1	9.5	0.987

**Notes.**<sup>a</sup>The notation of D or T represents doublet and triplet, respectively.<sup>b</sup>The right ascension and declination indicate the most probable direction determined by the fit.<sup>c</sup>The superscripts indicate events that are shared by other multiplets.<sup>d</sup>The time difference  $\Delta T$  is the time interval between the first and the last neutrino event.<sup>e</sup>The local p-values are introduced in the main text and converted to the corresponding FAR per year.**Figure 5.** Distribution of the TS-score converted into the corresponding FAR. Blue circles, red triangles, and white empty markers represent doublets, triplets, and combined distributions of experimental data by the TS-score, while the black line represents the expectation from backgrounds. The right panel provides an enlarged view of the large significance region. The vertical dashed line in the right panel corresponds to the inverse of live time of  $1/11.4 \text{ yr}^{-1}$ .

terminated thresholds of  $\text{FAR} = 1 \text{ yr}^{-1}$ . Because some doublets and triplets share the same events, the 12 multiplets point to seven unique directions in the Northern Sky. Note that each local p-value listed in the table is obtained directly from the PDF of the TS score. The post-trial global p-value is obtained by  $1 - (1 - p_{\text{local}})^N$ , that is, the probability that at least one doublets or triplets has a local p-value smaller than  $p_{\text{local}}$  in the  $N$  multiplet pool. The most significant multiplet ( $k = 1$ ) has a post-

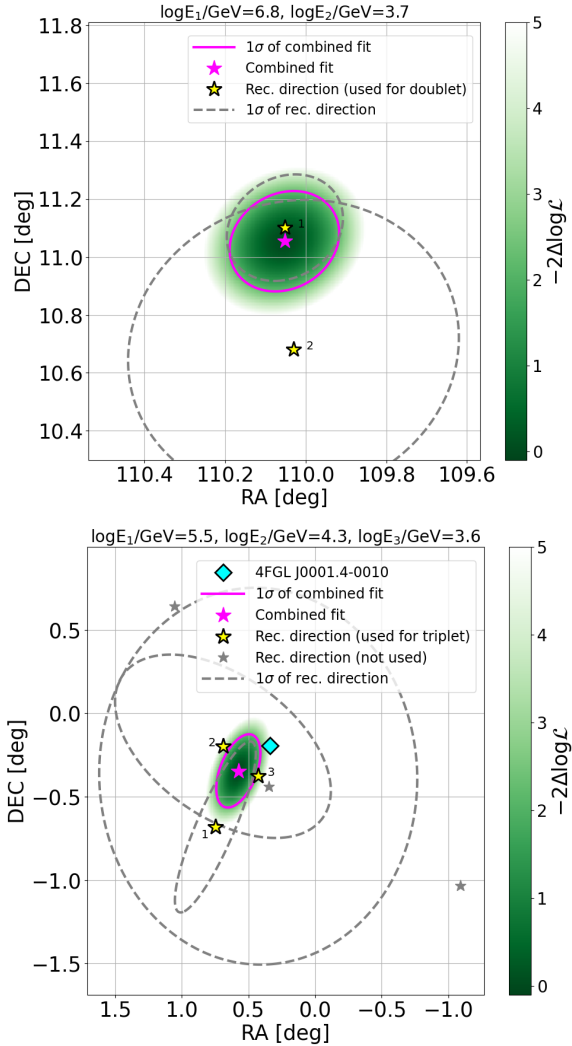
trial global p-value of 0.32, corresponding to a FAR of  $0.034 \text{ yr}^{-1}$ .

To probe any statistical deviation from the background-only hypothesis in the dataset as a whole, we perform a binomial test (see Appendix) for the 12 multiplets, and the p-value evaluated by the pseudo-experiment is 0.38. Thus, for the entire dataset, the observation is consistent with the background-only hypothesis.

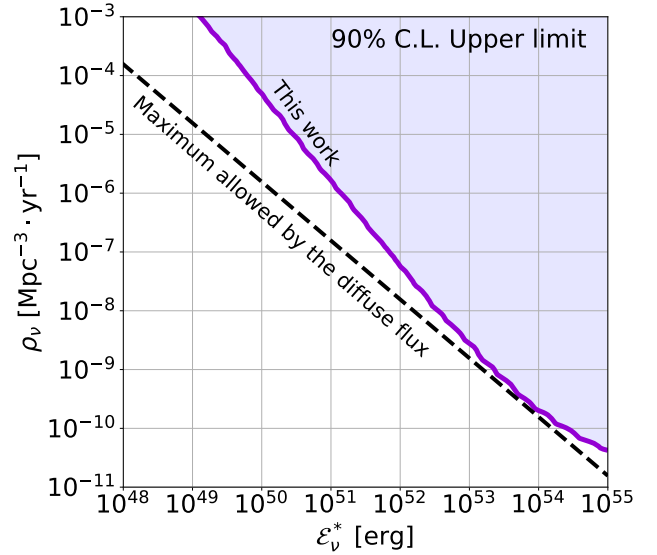
Figure 6 illustrates the contours of the top two significant multiplets  $k = 1$  and  $k = 2$ , as shown in the upper and lower panels, respectively. The  $k = 1$  multiplet emerges as a significant doublet, because one of the reconstructed energies is very high at 6 PeV (previously reported in Aartsen et al. (2016b,c)).

The null detection of statistically significant multiplets constrains the parameters of  $\mathcal{E}_\nu^*$  and  $\rho_\nu$ . We use the largest  $\Lambda = 23.5$  (*i.e.*, the highest inconsistency with the background-only hypothesis) found in the dataset, considering that a multiplet exceeding this value favors an astrophysical origin. For given  $(\mathcal{E}_\nu^*, \rho_\nu)$ , we inject neutrinos with a power law of  $E^{-2.3}$  from 10 TeV to 1 PeV and zero elsewhere, and calculate how often it records a multiplet larger than this value in the observation. A set of parameters with a frequency higher than 0.9 is ruled out at a 90 % confidence level. Figure 7 shows the contours of the neutrino transient source parameters  $(\mathcal{E}_\nu^*, \rho_\nu)$  at the 90% confidence level for the  $E^{-2.3}$  spectrum. The area above the curve is excluded at the 90% confidence level.





**Figure 6.** The contour plots of the direction of the two most significant multiplets. The upper and lower panels represent the doublet ( $k = 1$ ) and the triplet ( $k = 2$ ), respectively. Yellow stars indicate the directions of neutrino events to form the multiplets, while magenta stars denote the fitted directions of the multiplets. The dashed lines outline 68% containment uncertainty regions of each event determined by assuming Gaussian distribution, while magenta solid lines represent that of the fitted directions. The background color scales represent the residuals of the signal likelihoods:  $-2\Delta \log \mathcal{L}^{\text{sig}}$ . Small gray stars in the bottom panel represent neutrino events observed around the time of multiplet detection (from MJD59007 to MJD59047), but are not included in the multiplet found by the seed event method (see Sec. 3.1). In the lower panel, the cyan diamond represents the direction of a Fermi source 4FGL J0001.4-0010 (Ballet et al. 2023), which is separated by  $0.28^\circ$  from the best fit direction.



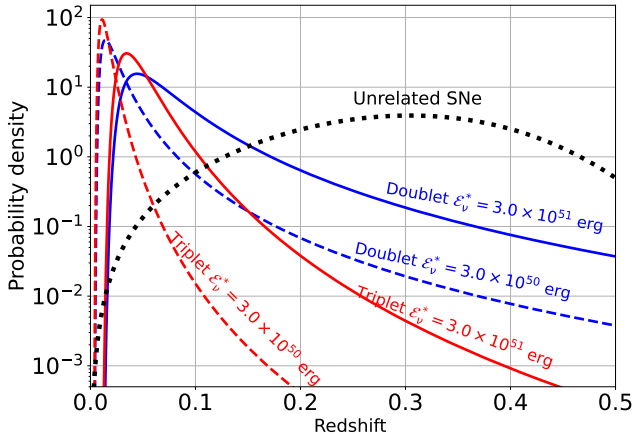
**Figure 7.** Contours of excluded region of neutrino transient source parameters ( $\mathcal{E}_\nu^*$ ,  $\rho_\nu$ ) at 90% confidence level when  $\Delta T_{\text{max}} = 30$  days, and the spectral indices are 2.3. The area above the curves is excluded at the 90% confidence level. The diagonal lines correspond to upper limits implied from the diffuse flux when the signal source spectrum is  $\gamma = 2.3$ . These diffuse flux constraints are determined so as not to overshoot the energy distribution of the measured diffuse neutrino flux (Abbasi et al. 2022a) (see Sec. 5.1). All the constraints are obtained assuming the SFR compatible evolution.

## 5. DISCUSSION

### 5.1. Relationship with constraints by the diffuse neutrino flux

Transient sources should also contribute to the diffuse neutrino flux and their contributions must be less than the total observed diffuse flux intensity, resulting in parameter constraints on  $(\mathcal{E}_\nu^*, \rho_\nu)$  (Murase & Waxman 2016; Yoshida et al. 2022). The diagonal line in Fig. 7 corresponds to the maximally allowed limit of the partial contributions of transient source fluxes implied from the diffuse neutrino flux assuming  $\gamma = 2.3$ . Note that this value is towards the lower range of spectral indices inferred from the diffuse flux by IceCube. The upper bound is determined by requiring that the assumed flux does not exceed the IceCube track limit (as a benchmark of the flux, we are using the flux level  $\phi_{@100 \text{ TeV}}^{\nu_\mu + \bar{\nu}_\mu} = 1.44 \times 10^{-18} \text{ GeV}^{-1} \text{ cm}^{-2} \text{ sec}^{-1} \text{ sr}^{-1}$  and  $\gamma = 2.37$  (Abbasi et al. 2022a)). With present sensitivity, the constraint by the multiplet analysis is weaker than the interpretation of the measured diffuse flux.

### 5.2. Posterior analysis of higher-rank multiplets



**Figure 8.** Probability density of the redshift distributions of neutrino sources detected as 30 days doublet (blue) and triplet (red) in the direction of the observed triplet ( $k = 2$  in Table 1) for neutrino emission energies of  $3 \times 10^{50}$  erg (dashed) and  $3 \times 10^{51}$  erg (solid). The black dotted curve represents the distribution of the unrelated closest SNe with a burst rate density of  $10^{-4} \text{ Mpc}^{-3} \text{ yr}^{-1}$  observed during 30 days and a solid angle of  $\Delta\Omega_\nu = \pi \cdot (0.3^\circ)^2$  (Yoshida et al. 2022).

As mentioned in Sec. 4, several multiplets share common neutrino events. In general, when more than three neutrino events form a multiplet, the subsets can become multiple doublets. In particular, multiplets numbered  $k = 2, 7$  and  $k = 3, 5$  formed quadruplets within 30 days. The significance of the quadruplets are calculated a posteriori. The TS is similarly extended to higher-rank multiplets and the local p-value is defined as an upper percentile of the TS distribution in the scrambled dataset. The two quadruplets have post-trial global p-values of 0.57 and 0.27, respectively, and they are consistent with backgrounds. Moreover, these are the two most significant quadruplets in the entire dataset.

### 5.3. Multi-messenger astronomy using the neutrino multiplets

Searches for the astrophysical counterparts of neutrino multiplets by multi-messenger observations are a powerful strategy for the identification of high-energy neutrino transient sources. It has been pointed out (Strotjohann, Nora Linn et al. 2019; Yoshida et al. 2022) that neutrino multiplet detections effectively limit the detectable distance of neutrino sources, thereby provides a chance to evaluate a physical association. For example, a posteriori, we find that a Fermi source 4FGL J0001.4-0010 (Abdollahi et al. 2022; Ballet et al. 2023) is within 90% of containment uncertainty region of the  $k = 2$  triplet (within  $0.3^\circ$  of the fitted direction, see Fig. 6). The host galaxy FBQS J0001-0011 was identified as

a BL Lac (Véron-Cetty & Véron 2006) with its redshift of  $z = 0.46$  (Albareti et al. 2017). The probability of random coincidence in finding a Fermi source within this region is estimated to be approximately 5% based on the local number density of the Fermi sources. Given that the typical density of BL Lac is  $O(10^{-7}) \text{ Mpc}^{-3}$  (Ajello et al. 2013), the effective rate density in 30 days is  $\rho_\nu \sim 10^{-6} \text{ Mpc}^{-3} \text{ yr}^{-1}$  which gives constraint on  $\mathcal{E}_\nu^* < 3 \times 10^{51}$  erg from Fig. 7. Figure 8 shows the PDF of the redshift of transient sources for two cases  $\mathcal{E}_\nu^* = 3 \times 10^{50}$  erg and  $3 \times 10^{51}$  erg. The observed redshift of FBQS J0001-0011 is unlikely as a source of the triplet. Similarly, even if other frequent triplet. Similarly, even if other frequent transients such as type-Ia SNe (as shown by the dotted curve) are observed in the direction of the observed multiplets by other follow-up studies, they are also unlikely if  $z \gtrsim 0.1$ .

It has been argued that bright TeV-PeV neutrino sources could be related to bright X-ray sources with a high opacity to  $\gamma$ -rays (Murase et al. 2016). Motivated by this scenario, we perform a correlation analysis using publicly available data recorded by the Monitor of All-sky X-ray Images (MAXI) (Matsuoka et al. 2009). The X-ray signals were detected using Gas Slit Cameras (GSC) with a sensitive energy range from 2 keV to 20keV. The point spread function of the GSC is approximately 1 degree. The operation period entirely covers the range when the data in the present analysis is taken. We focus on X-ray photons ranging from 4 keV to 10 keV due to the high detection efficiency of GSCs and a relatively low background rate (Hiroi et al. 2011). The noise detected in GSCs originates from accidental hits of charged particles and the rate depends on the time. To cancel out time-dependent noise, we define the signal and control regions in the vicinities of the neutrino multiplet directions as a  $1.5^\circ$  circle and a  $3.0^\circ$  doughnut shape with inner radius of  $1.5^\circ$ , respectively, and calculate the X-ray flux as the difference between these regions. The statistical uncertainty of the flux is estimated by propagating Poisson fluctuations of the photon counts in both regions. No significant X-ray emission is observed beyond the noise level in association with the detected neutrino multiplets, and thereby 90% CL upper limits on the average X-ray energy flux over  $\Delta T$  are placed in each of the multiplets except for  $k = 8$  and  $k = 12$  (no X-ray data available). The upper limits of the X-ray energy flux is approximated as

$$F_X < 8 \times 10^{-11} \left( \frac{\Delta T}{\text{day}} \right)^{-1/2} \text{ erg cm}^{-2} \text{ s}^{-1} \quad (6)$$

at the 90% CL.

## 6. CONCLUSION

We present a search for high-energy neutrino multiplets on the timescale of 30 days using 11.4 years of IceCube data. Dedicated search algorithms and likelihood constructions are developed to optimize the month-scale transient phenomena. No significant doublets or triplets are observed, providing constraints on bright but rare source populations. The upper limit is weaker than the constraint based on the measured diffuse flux by the IceCube.

Future multi-messenger observations using neutrino multiplet detections as well as high statistical searches brought about by future neutrino detectors such as IceCube-Gen2 (Aartsen et al. 2021b) are promising for understanding high-energy neutrino emission mechanisms.

### ACKNOWLEDGEMENTS

The IceCube collaboration acknowledges the significant contributions to this manuscript from Nobuhiro Shimizu. The authors gratefully acknowledge the support from the following agencies and institutions: USA – U.S. National Science Foundation-Office of Polar Programs, U.S. National Science Foundation-Physics Division, U.S. National Science Foundation-EPSCoR, U.S. National Science Foundation-Office of Advanced Cyberinfrastructure, Wisconsin Alumni Research Foundation, Center for High Throughput Computing (CHTC) at the University of Wisconsin-Madison, Open Science Grid (OSG), Partnership to Advance Throughput Computing (PATH), Advanced Cyberinfrastructure Coordination Ecosystem: Services & Support (ACCESS), Frontera computing project at the Texas Advanced Computing Center, U.S. Department of Energy-National Energy Research Scientific Computing Center, Particle astrophysics research computing center at the University of Maryland, Institute for Cyber-Enabled Research at Michigan State University, Astroparticle physics computational facility at Marquette University, NVIDIA Corporation, and Google Cloud Platform; Belgium – Funds for Scientific Research (FRS-FNRS and FWO), FWO Odysseus and Big Science programmes, and Belgian Federal Science Policy Office (Belspo); Germany – Bundesministerium für Bildung und Forschung (BMBF), Deutsche Forschungsgemeinschaft (DFG), Helmholtz Alliance for Astroparticle Physics (HAP), Initiative and Networking Fund of the Helmholtz Association, Deutsches Elektronen Synchrotron (DESY), and High Performance Computing cluster of the RWTH Aachen; Sweden – Swedish Research Council, Swedish Polar Research Secretariat, Swedish National Infrastructure for Computing (SNIC),

and Knut and Alice Wallenberg Foundation; European Union – EGI Advanced Computing for research; Australia – Australian Research Council; Canada – Natural Sciences and Engineering Research Council of Canada, Calcul Québec, Compute Ontario, Canada Foundation for Innovation, WestGrid, and Digital Research Alliance of Canada; Denmark – Villum Fonden, Carlsberg Foundation, and European Commission; New Zealand – Marsden Fund; Japan – Japan Society for Promotion of Science (JSPS) and Institute for Global Prominent Research (IGPR) of Chiba University; Korea – National Research Foundation of Korea (NRF); Switzerland – Swiss National Science Foundation (SNSF).

### APPENDIX BINOMIAL P-VALUE

Suppose that there are  $N$  local p-values  $\{p_1, p_2, \dots, p_N\}$  that are sorted in ascending order (from the smallest to the largest):  $\{q_1, q_2, \dots, q_N\}$ . Under the background-only hypothesis,  $k$ -th smallest p-value,  $x = q_k$ , is distributed as

$$\rho_k(x) = k \binom{N}{k} x^{k-1} (1-x)^{N-k}, \quad (7)$$

such that the p-value of each  $q_k$  is given as a cumulative distribution function, as in

$$P(k) = \int_0^{q_k} \rho_k(x) dx = k \binom{N}{k} B_{q_k}(k, N-k+1), \quad (8)$$

where  $B_x(a, b) = \int_0^x t^{a-1} (1-t)^{b-1} dt$  is an incomplete beta function. By integrating by parts, this can be expressed in a different form:

$$P(k) = \sum_{m=k}^N \binom{N}{m} q_k^m (1-q_k)^{N-m}, \quad (9)$$

and are sometimes referred to as binomial p-values. Note that these quantities are *trial-corrected* (i.e.,  $P(k)$  is uniformly distributed in  $(0, 1)$  if  $p_k$  ( $k = 1, 2, \dots, N$ ) is also uniformly distributed). In particular, from Eq. (9), the p-value of the most significant observation ( $q_1$ ) is calculated as  $P(1) = 1 - (1 - q_1)^N$ , which is the trial-corrected global p-value introduced in Sec. 4.

To define the significance of the entire dataset, the smallest binomial p-value  $\min P(k)$  in subsets  $\{P(1), P(2), \dots, P(M)\}$  ( $M = 12$  as shown in Table 1) can be used. This  $\min P(k)$  cannot be interpreted as a p-value, thus the distribution of  $\min P(k)$  is numerically evaluated by pseudo-experiments, and a lower percentile of the distribution is computed to define the p-value for the observed  $\min P(k)$ .

## REFERENCES

- Aartsen, M., et al. 2015, *Astroparticle Physics*, 66, 39, doi: <https://doi.org/10.1016/j.astropartphys.2015.01.001>
- . 2017a, *Journal of Instrumentation*, 12, P03012, doi: [10.1088/1748-0221/12/03/P03012](https://doi.org/10.1088/1748-0221/12/03/P03012)
- Aartsen, M. G., et al. 2008, *Astroparticle Physics*, 29, 299, doi: <https://doi.org/10.1016/j.astropartphys.2008.02.007>
- . 2013, *Phys. Rev. Lett.*, 111, 021103, doi: [10.1103/PhysRevLett.111.021103](https://doi.org/10.1103/PhysRevLett.111.021103)
- . 2016a, *Journal of Instrumentation*, 11, P11009, doi: [10.1088/1748-0221/11/11/P11009](https://doi.org/10.1088/1748-0221/11/11/P11009)
- . 2016b, *The Astrophysical Journal*, 833, 3, doi: [10.3847/0004-637X/833/1/3](https://doi.org/10.3847/0004-637X/833/1/3)
- . 2016c, *Phys. Rev. Lett.*, 117, 241101, doi: [10.1103/PhysRevLett.117.241101](https://doi.org/10.1103/PhysRevLett.117.241101)
- . 2017b, *The Astrophysical Journal*, 835, 45, doi: [10.3847/1538-4357/835/1/45](https://doi.org/10.3847/1538-4357/835/1/45)
- . 2018, *Science*, 361, eaat1378, doi: [10.1126/science.aat1378](https://doi.org/10.1126/science.aat1378)
- . 2019, *Phys. Rev. Lett.*, 122, 051102, doi: [10.1103/PhysRevLett.122.051102](https://doi.org/10.1103/PhysRevLett.122.051102)
- . 2020, *Phys. Rev. Lett.*, 125, 121104, doi: [10.1103/PhysRevLett.125.121104](https://doi.org/10.1103/PhysRevLett.125.121104)
- . 2021a, *Nature*, 591, 220, doi: [10.1038/s41586-021-03256-1](https://doi.org/10.1038/s41586-021-03256-1)
- . 2021b, *J. Phys. G*, 48, 060501, doi: [10.1088/1361-6471/abb4d8](https://doi.org/10.1088/1361-6471/abb4d8)
- Abbasi, R., et al. 2009, *Nuclear Instruments and Methods in Physics Research Section A: Accelerators, Spectrometers, Detectors and Associated Equipment*, 601, 294, doi: <https://doi.org/10.1016/j.nima.2009.01.001>
- . 2010, *Nuclear Instruments and Methods in Physics Research Section A: Accelerators, Spectrometers, Detectors and Associated Equipment*, 618, 139, doi: <https://doi.org/10.1016/j.nima.2010.03.102>
- . 2013, *Nuclear Instruments and Methods in Physics Research Section A: Accelerators, Spectrometers, Detectors and Associated Equipment*, 703, 190, doi: <https://doi.org/10.1016/j.nima.2012.11.081>
- . 2021, *Phys. Rev. D*, 104, 022002, doi: [10.1103/PhysRevD.104.022002](https://doi.org/10.1103/PhysRevD.104.022002)
- . 2022a, *The Astrophysical Journal*, 928, 50, doi: [10.3847/1538-4357/ac4d29](https://doi.org/10.3847/1538-4357/ac4d29)
- . 2022b, *Science*, 378, 538, doi: [10.1126/science.abg3395](https://doi.org/10.1126/science.abg3395)
- . 2023a, *Science*, 380, 1338, doi: [10.1126/science.adc9818](https://doi.org/10.1126/science.adc9818)
- . 2023b, *The Astrophysical Journal Supplement Series*, 269, 25, doi: [10.3847/1538-4365/acfa95](https://doi.org/10.3847/1538-4365/acfa95)
- Abdollahi, S., et al. 2022, *The Astrophysical Journal Supplement Series*, 260, 53, doi: [10.3847/1538-4365/ac6751](https://doi.org/10.3847/1538-4365/ac6751)
- Ahrens, J., et al. 2004, *Nuclear Instruments and Methods in Physics Research Section A: Accelerators, Spectrometers, Detectors and Associated Equipment*, 524, 169, doi: <https://doi.org/10.1016/j.nima.2004.01.065>
- Ajello, M., et al. 2013, *The Astrophysical Journal*, 780, 73, doi: [10.1088/0004-637X/780/1/73](https://doi.org/10.1088/0004-637X/780/1/73)
- Albaret, F. D., et al. 2017, *ApJS*, 233, 25, doi: [10.3847/1538-4365/aa8992](https://doi.org/10.3847/1538-4365/aa8992)
- Ballet, J., Bruel, P., Burnett, T. H., & Lott, B. 2023, *Fermi Large Area Telescope Fourth Source Catalog Data Release 4 (4FGL-DR4)*. <https://arxiv.org/abs/2307.12546>
- Gal-Yam, A. 2019, *Annual Review of Astronomy and Astrophysics*, 57, 305, doi: <https://doi.org/10.1146/annurev-astro-081817-051819>
- Hayasaki, K., & Yamazaki, R. 2019, *The Astrophysical Journal*, 886, 114, doi: [10.3847/1538-4357/ab44ca](https://doi.org/10.3847/1538-4357/ab44ca)
- Hiroi, K., et al. 2011, *Publications of the Astronomical Society of Japan*, 63, S677, doi: [10.1093/pasj/63.sp3.S677](https://doi.org/10.1093/pasj/63.sp3.S677)
- Kheirandish, A., & Murase, K. 2023, *The Astrophysical Journal Letters*, 956, L8, doi: [10.3847/2041-8213/acf84f](https://doi.org/10.3847/2041-8213/acf84f)
- Kintscher, T. 2020, PhD thesis, Humboldt-Universität zu Berlin, Mathematisch-Naturwissenschaftliche Fakultät, doi: <http://dx.doi.org/10.18452/21948>
- Kowalski, M., & Mohr, A. 2007, *Astroparticle Physics*, 27, 533, doi: <https://doi.org/10.1016/j.astropartphys.2007.03.005>
- Matsuoka, M., et al. 2009, *Publications of the Astronomical Society of Japan*, 61, 999, doi: [10.1093/pasj/61.5.999](https://doi.org/10.1093/pasj/61.5.999)
- Moriya, T. J., Sorokina, E. I., & Chevalier, R. A. 2018, *Space Science Reviews*, 214, 59, doi: [10.1007/s11214-018-0493-6](https://doi.org/10.1007/s11214-018-0493-6)
- Murase, K. 2018, *Phys. Rev. D*, 97, 081301, doi: [10.1103/PhysRevD.97.081301](https://doi.org/10.1103/PhysRevD.97.081301)
- Murase, K., Guetta, D., & Ahlers, M. 2016, *Phys. Rev. Lett.*, 116, 071101, doi: [10.1103/PhysRevLett.116.071101](https://doi.org/10.1103/PhysRevLett.116.071101)
- Murase, K., Kimura, S. S., Zhang, B. T., Oikonomou, F., & Petropoulou, M. 2020, *The Astrophysical Journal*, 902, 108, doi: [10.3847/1538-4357/abb3c0](https://doi.org/10.3847/1538-4357/abb3c0)
- Murase, K., Thompson, T. A., Lacki, B. C., & Beacom, J. F. 2011, *Phys. Rev. D*, 84, 043003, doi: [10.1103/PhysRevD.84.043003](https://doi.org/10.1103/PhysRevD.84.043003)
- Murase, K., & Waxman, E. 2016, *Phys. Rev. D*, 94, 103006, doi: [10.1103/PhysRevD.94.103006](https://doi.org/10.1103/PhysRevD.94.103006)
- Pitik, T., Tamborra, I., Lincetto, M., & Franckowiak, A. 2023, *Monthly Notices of the Royal Astronomical Society*, 524, 3366, doi: [10.1093/mnras/stad2025](https://doi.org/10.1093/mnras/stad2025)
- Stein, R., et al. 2021, *Nature Astronomy*, 5, 510, doi: [10.1038/s41550-020-01295-8](https://doi.org/10.1038/s41550-020-01295-8)



Strotjohann, Nora Linn, Kowalski, Marek, & Franckowiak, Anna. 2019, *A&A*, 622, L9,  
doi: [10.1051/0004-6361/201834750](https://doi.org/10.1051/0004-6361/201834750)  
Véron-Cetty, M.-P., & Véron, P. 2006, PhD thesis,  
doi: <https://doi.org/10.1051/0004-6361:20065177>  
Winter, W., & Lunardini, C. 2023, *The Astrophysical Journal*, 948, 42, doi: [10.3847/1538-4357/acbe9e](https://doi.org/10.3847/1538-4357/acbe9e)

Yoshida, S., Murase, K., Tanaka, M., Shimizu, N., &  
Ishihara, A. 2022, *The Astrophysical Journal*, 937, 108,  
doi: [10.3847/1538-4357/ac8dfd](https://doi.org/10.3847/1538-4357/ac8dfd)